



Norwegian University of
Science and Technology

Videreutvikling system for posisjonering/DP

test av prototyp system med øyesikker 1550
nm laser diode/fiber laser teknologi

Iselin Silvana Haugen Neteland

Master of Science in Electronics

Submission date: September 2017

Supervisor: Ulf Lennart Østerberg, IES

Co-supervisor: John Klepsvik, Kongsberg Seatex AS

Norwegian University of Science and Technology
Department of Electronic Systems

Summary

This master work deals with investigating a laser based range finding system. The laser has a wavelength of 1 550 nm and the system will be comparable to SpotTrack, which uses 905 nm. This paper will build on the work that was done in the autumn of 2016, where investigations were carried out to find out which lens would be the best option to use together with a diode laser, an acylindrical or a cylindrical lens [1]. The conclusion there was that the acylindrical lens would be the better option. That solution has been incorporated in to this work.

This work has focused on what combinations of laser and detector would be the best option do develop further, if that even is a good option. This has been based on eye safety evaluations, costs of laser and detector compared to the those of SpotTrack and how well the system performs compared to SpotTrack. Two kinds of lasers were considered, fiberlaser and diode laser. Fiber lasers will be able to send out higher power and a more narrow beam, but are very costly. Diode laser are cheaper, but have a larger beam divergence, which will reduce the range. The detectors that were looked into were pin detector and avalanche photodiode (APD). Here too, the choice was between costs and performance. Pin detectors are generally less sensitive, but cheap compared to APDs. APDs have high sensitivity, but will easily become expensive.

These factors were weighed against each other and compared. The finding was that a combination consisting of a laser diode and an APD would be the best option to develop further seeing that the range would be good and the increase in costs moderate. Furthermore, a laser system with a laser diode giving out strength would be more eye-safe than a fiber laser on full strength.

Samandrag

Denne masteroppgåva tek føre seg arbeidet med å undersøke eit laserbasert avstandsmålingssystem. Laseren har bølgelengda 1 550 nm og systemet vil vere samanliknbart med SpotTrack, som bruker 905 nm. Denne oppgåva byggjer vidare på arbeidet gjort hausten 2016, der det blei gjort undersøkingar for å finne ut kva type linse som ville vere best å bruke saman med ein diodelaser, asylindrisk eller sylindrisk [1]. Det blei der konkludert med at det beste valget var å bruke ei asylindrisk linse. Den har blitt brukt vidare i dette arbeidet.

Dette arbeidet har fokusert på å finne ut kva for ein kombinasjon av laser og detektor som ville vere mest fordelaktig å vidareutvikle, om det i det heile tatt er det. Det er basert på tryggleiksvurderingar med omsyn til augeskader, kostandar med å kjøpe inn laser og detektor samanlikna med SpotTrack og kor godt systemet presterer samanlikna med SpotTrack. To typar laser blei vurdert, fiberlaser og laserdiode. Fiberlasere kan gje ut større effekt og smalere stråler, men er svært kostbare. Diodelasere er billigere, men har større stråledivergens, som reduserer rekkevidda. Detektorene som blei undersøkt var pin-detektor og avalanche photodiode (APD). Her òg sto det mellom kostnad og ytelse. Pin-detektorar er mindre sensitive, men billige samanlikna med APD. APD har svært god sensitivitet, men blir fort dyre.

Desse faktorane blei veigd opp mot kvarandre og samanlikna. Det blei funnet at ein kombinasjon av laserdiode og APD ville vere det mest fornuftige å gå vidare med ettersom rekkevidda vil vere god og kostnadsauka moderat. Dessutan vil eit system med ein laserdiode på full styrke ha større augetryggleik enn ein fiberlaser på full styrke.

Preface

This thesis covers the work carried out during the the spring of 2017. This work centred around evaluating a laser-detector combination for further development of a laser based ranging system similar to the SpotTrack. The evaluation covers the areas of theoretical calculation of range, costs and eye safety as well as practical testing of the options. This work was done in collaboration with Kongsberg Seatex AS who provided me with the prototype system I was working on and all the other equipment I would need.

I would like to thank my supervisors, Ulf Lennart Østerberg at NTNU and John Oddvar Klepsvik at Kongsberg Seatex AS for giving me the opportunity to work on this project and all help and support throughout this period. I would also like to thank Sigbjørn Egge and other employees at Kongsberg Seatex AS for always being helpful and supportive and finally Sondre Schwenke and Achim Gerstenberg who brightened up the empty office during the summer.

Contents

Summary	i
Samandrag	ii
Preface	iii
Table of Contents	vi
List of Tables	vii
List of Figures	x
Abbreviations	xi
Mathematical notation	xiii
1 Introduction	1
2 Theory	3
2.1 Atmospheric conditions	3
2.1.1 Scattering	3
2.1.2 Absorption	5
2.2 Range of a laser system/The range equation	7
2.2.1 Spatial distribution	8
2.2.2 The target, a corner cube retroreflector	9
2.2.3 Receiver, detector and noise	11
2.3 Signal to noise ratio	12
2.3.1 Statistics of the sensor output signal	13
2.3.2 Probability of detection and false alarm	13

2.3.3	Determining the minimum value of SNR	15
2.4	Laser safety	16
2.5	Figure of merit	17
3	Theoretical calculations	19
3.1	Range	19
3.2	Results of safety calculations	27
3.3	FOM and costs calculations	27
4	Experiment	29
4.1	experimental work	29
4.2	Experimental results	34
5	Discussion	37
6	Conclusion	39
	Bibliography	41

List of Tables

2.1	Different weather conditions and their attenuation	5
2.2	Arguments and results for $g(y)$	16
3.1	Characteristics for two kinds of lasers with 1550 nm wavelength, a diode laser (LD) and a fiber laser (FL).	20
3.2	The target, a corner cube retroreflector.	20
3.3	Receiver lens characteristics, identical for all three laser systems.	22
3.4	Detectors with amplifiers	22
3.5	The three combinations and their properties.	22
3.6	The costs and the FOM for four different combinations.	28
4.1	Input power to the FL versus the average output power, P_{avg} emitted by the fiber laser.	31

List of Figures

2.1	Atmospheric transmission over 1 NM sea level path. [2]	4
2.2	Transmittance of electromagnetic waves in the atmosphere. [2]	4
2.3	Absorption spectrum of a mix of equal parts of O ₂ , CO ₂ CH ₄ and N ₂ O. [3]	5
2.4	Attenuation of light caused by maritime aerosols	6
2.5	Attenuation of light caused by rural aerosols	6
2.6	Attenuation of light caused by urban aerosols	7
2.7	1/e ² width in red and FWHM in green for a Gaussian distribution. [4]	8
2.8	Illustration showing how a corner reflector works. The Illustrations shows two rays, red and black being reflected from different directions. Each ray is reflected three times.	10
2.9	PDF of three signals of different strengths and noise PDF. [5]	14
2.10	MPE versus wavelength for different exposure times (pulse durations)	17
3.1	Power reflected onto the detector for the FL and APD combination for five different visibilities.	21
3.2	Voltage output for the FL and APD combination for five different visibilities. Pink colours represent detector gain of 4, and green/blue colours represent a gain of 20.	21
3.3	Power reflected onto the detector for the LD and APD combination for five different visibilities.	23
3.4	Voltage output for the LD and APD combination for five different visibilities.	23
3.5	Power reflected onto the detector for the FL and pin combination for five different visibilities.	24

3.6	Voltage output for the FL and pin combination for five different visibilities.	24
3.7	Power reflected onto the detector for the LD and APD combination if P_t is 30 W, under five different weather conditions. Detection threshold included.	25
3.8	Voltage output from the the detector in the LD and APD combination if P_t is 30 W and $M = 20$, under five different weather conditions.	26
4.1	The fiber laser and APD mounted on the prototype.	29
4.2	The fiber laser and APD mounted on the prototype.	30
4.3	The diode laser and APD mounted on the prototype.	30
4.4	Upper front side of the prototype	31
4.5	The view from the prototype testing.	31
4.6	Input power to the FL versus the average output power, P_{avg} emitted by the fiber laser.	32
4.7	Trigger pulse and pulse from very close reflection.	33
4.8	Trigger pulse and returned pulse from target at 240 m distance. . .	33
4.9	Even though the signal on average is not enough to sturate the APD, some of them do.	34
4.10	Output signal from APD when averaged.	35
4.11	Peak voltage from FL and APD cobimation is 2.7 V	35
4.12	Minutes later the peak output signal is 4 V, without any noticeable change in weather. shows a maximum of 4 V of the returned pulse. .	36
4.13	Returned pulse from LD and APD combination when holding a sheet of paper in front of laser.	36

Abbreviations

APD Avalanche photodiode

FL Fiber laser

FOM Figure of merit

FWHM Full Width Half Maximum

IR Infrared

LD Laser diode

MPE Maximum permissible exposure

NEP Noise equivalent power

NOHD Nominal hazard distance

PDF Probability density function

PFA Probability of false alarm

RMS Root mean square

SNR Signal to noise ratio

ST SpotTrack (905 nm)

TI Gain Transimpedance gain

UV Ultraviolet

Mathematical notation

A_{cc} Target area

A_r Area of the receiver

A_{rtn} Area of the returned light beam

c The speed of light

C_5 Correction factor

d_A Diameter of aperture used to calculate exposure limits

d_{cc} Diameter of corner cube retroreflector

d_r Diameter of the receiver

E_p Energy in a single laser pulse

I_{target} Intensity at the distance of the target

P_d Probability of detection

$p_n(v)$ The noise PDF

$p_{s+n}(v)$ The noise PDF

P_{avg} Average power transmitted from the laser

P_t Pulse peak power

prf Pulse repetition frequency

P_r^{max} Maximum possible peak power on detector from the laser beam pulse at a given distance

t_w Pulse width

R Distance to the target

R_0 Detector responsivity

SNR_{min} The lowest SNR to fulfil the demands of P_d and PFA

t Time used before a laser signal is returned

T_{max} The duration of a complete exposure to the laser beam

v_s Voltage of a signal where a target is present

v_{th} Threshold for what voltage counts as a detection

w_h Beam width in the horizontal direction

w_v Beam width in the vertical direction

Δt Integration time of the detector

η Quantum efficiency of a detector

θ_h Angular divergence in the horizontal direction
 $\theta_{h,\text{FWHM}}$ Integration time of the detector
 θ_v Angular divergence in the vertical direction
 $\theta_{v,\text{FWHM}}$ Integration time of the detector
 $\theta_{cc}^{\text{diff}}$ Angle between the first minima of an Airy disk
 ρ_t Target surface reflectivity
 σ Attenuation coefficient
 $\sigma_{v,n}$ RMS value of the voltage pdf when there is no target present
 $\sigma_{v,s+n}$ RMS value of the voltage pdf when the target is present
 τ_0 Optical transmission of the receiver
 τ_a Atmospheric transmission

Introduction

Ranging systems are useful in many different situations. They appear in driver assistant systems in cars to keep a safe distance to the car in front and measure the distance between the earth and the moon. These systems can be based on many different technologies. One of them is to send laser pulses towards the target and measure the time they take to return. This is the technology used in measuring the distance to the moon and this is also the technology used in SpotTrack.

SpotTrack is used together with other technologies in dynamic positioning in areas such as port areas and near oil drilling platforms. A big advantage with using a system such as SpotTrack is its accuracy in knowing the distance to the target. A disadvantage is the wavelength currently in use. Safety considerations limits the range of the system as the maximum output power can give eye damages. There has been developed a prototype for a similar system but with a wavelength that is not as harmful for the eyes, 1 550 nm. A ranging system based on this wavelength would allow for higher output power, and as such, a longer range. A higher output and longer range could also open up new uses such as offshore windmill areas.

When developing such a system, there are many types of lasers and detectors that could be used. In this work, two laser technologies and two detector technologies that will be considered. The laser technologies are fiber laser (FL) and diode laser (LD). Fiber lasers will be able to give out higher peak powers and can give the system a very long range, but is generally expensive. Diode laser are cheaper, but have much less peak power. Even though the 1 550 nm is generally a safe wavelength, it can be harmful at high powers and will also be evaluated for both the lasers. The detectors that will be considered are pin detectors and avalanche photodiodes (APD). Here too, cost will be weight against performance as APDs generally have a much higher quantum efficiency than a pin detector, but is in return much more expensive.

Theory

2.1 Atmospheric conditions

A laser beam propagating through air will be absorbed and scattered, resulting in an attenuation of the power of the beam. This attenuation is wavelength dependent. For infrared light, it is caused by particles such as haze, dust, fog and cloud droplets, with haze particles and aerosols dominating near the earth's surface. [6] Figure 2.1 shows how electromagnetic waves of different wavelengths are attenuated by the atmosphere. Figure 2.2 zooms in on the infrared section and where it is clear that some wavelengths are heavily attenuated.

The transmission loss τ_a , caused by both scattering and absorption, can be determined using Beer's Law

$$\tau_a = \exp \left\{ - \int_0^R [a(R') + b(R')] dR' \right\} \quad (2.1)$$

This is simplified to an average value

$$\tau_a = \exp[-(a + b)R] = \exp(\sigma R). \quad (2.2)$$

Where σ is known as the attenuation coefficient.

An overview over what attenuation different weather conditions give can be found in table 2.1[7].

2.1.1 Scattering

Scattering happens when a molecule absorbs energy from a photon and immediately releases the energy again in all directions. There are two main types of scattering in the atmosphere, Mie and Rayleigh.

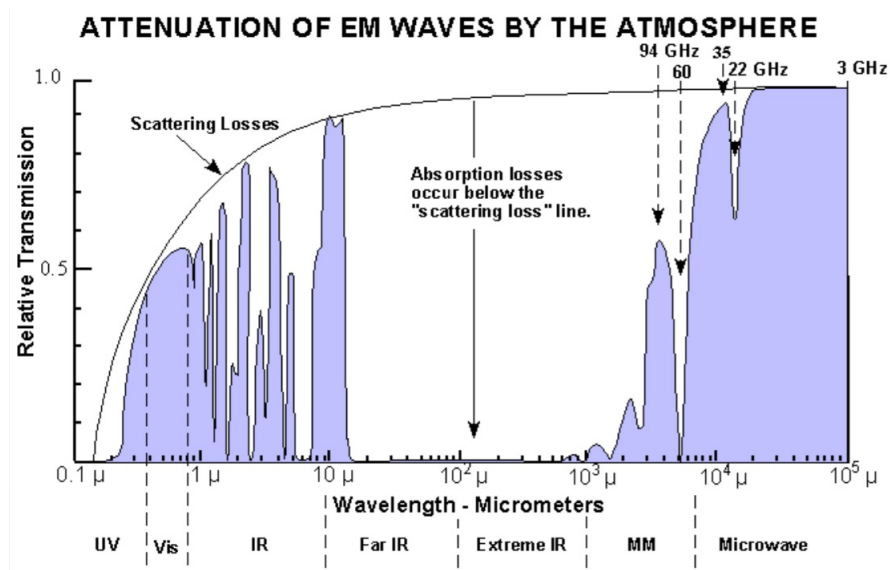


Figure 2.1: Atmospheric transmission over 1 NM sea level path. [2]

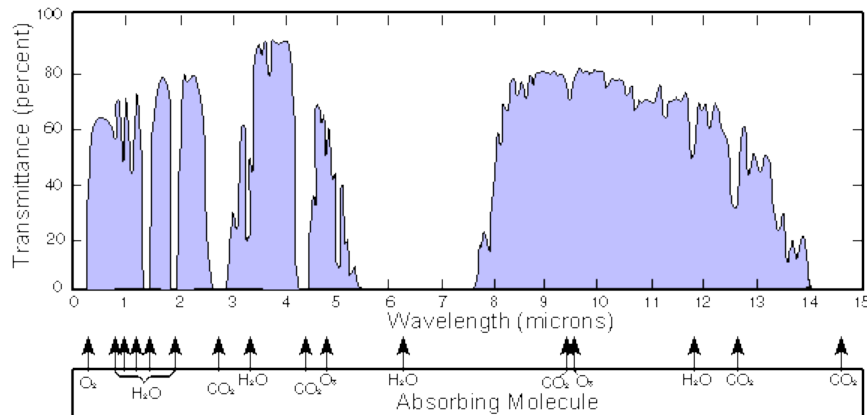


Figure 2.2: Transmittance of electromagnetic waves in the atmosphere. [2]

When light is scattered from molecules that are much smaller than the wavelength, it is called Rayleigh scattering. The scattering intensity depends on the size of the particles. Shorter wavelengths are scattered more strongly than longer wavelengths. This effect can be seen in figure 2.1.

Mie scattering is less wavelength dependent than Rayleigh scattering, but will dominate when the particles are the same size as, or larger, than the wavelength of the light. Mie scattering is responsible for the white light from mist and fog.

Table 2.1: Different weather conditions and their attenuation [7].

Condition	σ , [km^{-1}]	Visibility km	Precipitation mm/h
Clear	0,1	23,5	
Haze	0,4	5	
Light fog	2	1	
Moderat, fog	5	0,5	
Rain, drizzle	0,2	10	0,25
Rain, light	0,5	5	1
Rain, moderate	1,2	2	5
Rain, heavy	3,3	0,5	25
Snow, moderate	15	0,1	100

2.1.2 Absorption

When photons are absorbed by molecules in the atmosphere, their energy is transformed into internal energy and will eventually be transferred to other molecules in the atmosphere as heat[3]. Even though they are not the most abundant, particularly the greenhouse gasses, CO_2 , CH_4 , N_2O and water vapour will absorb light in distinct spectral regions, especially in the IR area. These specific absorption regions are due to the molecules' highly active vibration-rotation bands[6]. Except for water, these molecules have long lifetimes and are found evenly distributed across the whole earth, and so their effects do not vary much between regions. Their effects on attenuation in the IR region can be seen in figure 2.3.

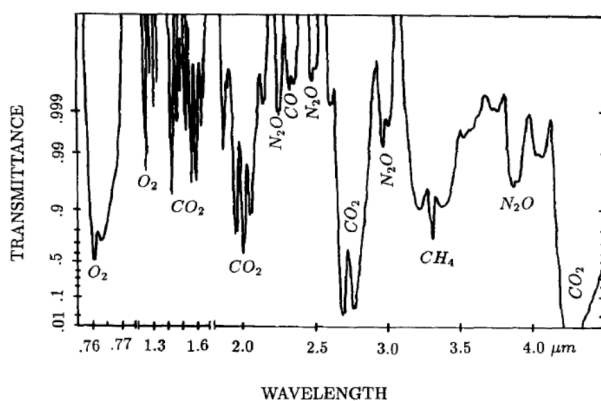


Figure 2.3: Absorption spectrum of a mix of equal parts of O_2 , CO_2 , CH_4 and N_2O . [3]

Other molecules can also contribute to light absorption depending on the wavelength and the atmospheric layer. Aerosols will also contribute strongly to the

absorption of light, especially in the visible, near UV and near IR spectra. The aerosol components can vary strongly across regions. Over oceans, there will be particles from sea salt. On land, dust and earth particles are important as well as organic materials from vegetation. In rural areas, the aerosols are a mix of water-soluble particles and dust like aerosols. Urban areas will, in addition to typical rural aerosols, contain aerosols from combustion processes and industrial sources[6]. Figures 2.5, 2.6 and 2.4 shows how different wavelengths can be attenuated differently in different regions.

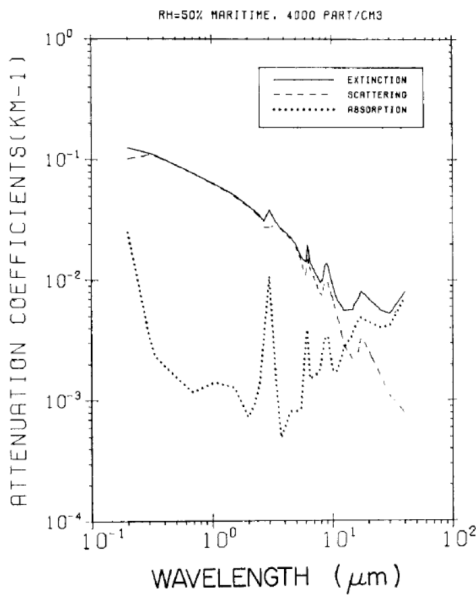


Figure 2.4: Attenuation of light caused by maritime aerosols [6].

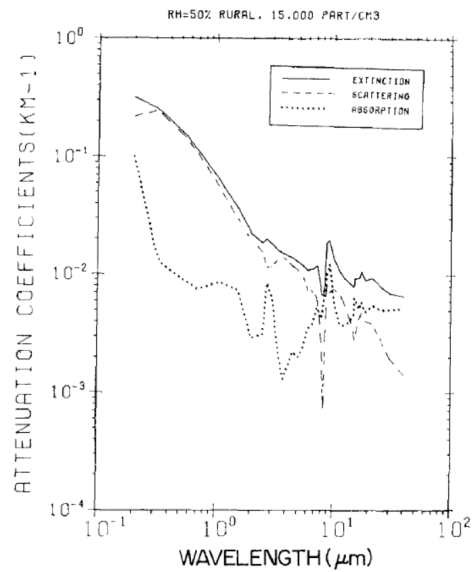


Figure 2.5: Attenuation of light caused by rural aerosols [6].

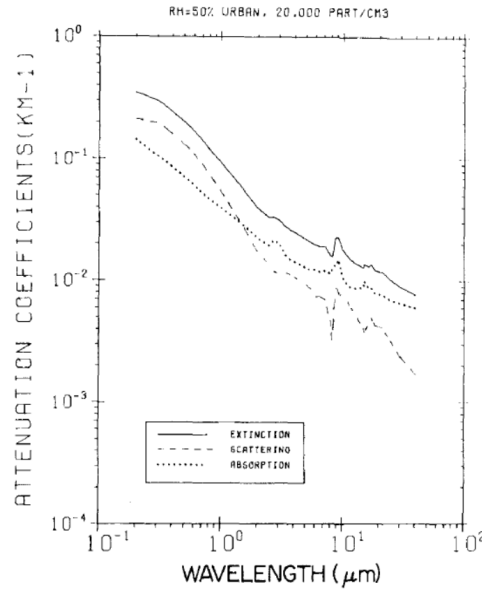


Figure 2.6: Attenuation of light caused by urban aerosols [6].

2.2 Range of a laser system/The range equation

The range of a laser ranging system is influenced by many factors. The transmitted power of the laser, the attenuation of the atmosphere, which has already been discussed, the divergence of the beam and target and detector characteristics are all important variables.

The laser transmits a signal and measures the time, t it takes before it returns after being reflected from an object. As the speed of light is known to be $c = 299\,792\,458$ m/s in vacuum, and close to that in air, it is easy to know the distance R to the object through this simple relation,

$$t = \frac{2R}{c}. \quad (2.3)$$

Using this expression, we can also see that a time delay of 1 nanosecond represents a distance of 0.15 meters and 100 ns represents 150 meters.

E_p is the energy contained in a single pulse. If we assume a simple model where the laser system fires short, rectangular pulses at regular intervals. The relationship between E_p , the average power P_{avg} and the pulse repetition frequency, prf is

$$E_p = \frac{P_{avg}}{prf}. \quad (2.4)$$

Pulse peak power is then

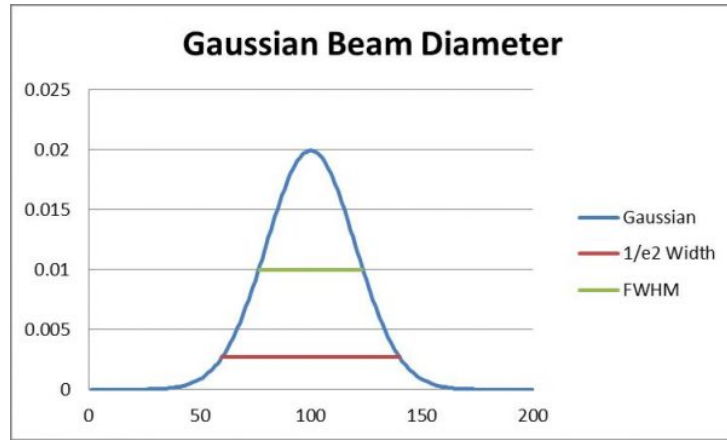


Figure 2.7: $1/e^2$ width in red and FWHM in green for a Gaussian distribution. [4]

$$P_t = \frac{E_p}{t_w}, \quad (2.5)$$

with t_w being the temporal pulse width.

2.2.1 Spatial distribution

The spatial shape of the laser beam is also important to consider. The distribution of the light can be similar to a Gaussian distribution, it can be nearly rectangular or have some other shape. The distribution can be the same in both the horizontal and vertical direction, or it can not be. As a Gaussian distribution does not have a strictly defined edge, there are a few different methods to define the width and radius of the beam. One is to use the full-width-half-maximum (FWHM) value. This is the diameter of the beam where the intensity has dropped to half of the peak intensity. A second method is to use the $1/e^2$ -radius, the radius of the beam where the intensity is $1/e^2$ of the peak. A third, and less commonly used method is to use the diameter at the $1/e^2$ -intensity of the beam. For a perfect Gaussian shape, the relationship between the $1/e^2$ -diameter and FWHM is

$$w_{1/e^2,diameter} = 1.6986 \cdot w_{FWHM}$$

Figure 2.7 illustrates these two definitions of the boundary.

When the shape is rectangular, it is common to define the diameter using FWHM. As the beam propagates through space, the area it covers will increase. The beam divergence describes this expansion in degrees or mrad.

Now, let us consider a fan shaped laser beam, where the horizontal distribution is Gaussian and the vertical distribution is rectangular. The intensity distribution, I_{target} reaching a target can be written as

$$I_{target} = I(x, y, R) = P_t \cdot \sqrt{\frac{8}{\pi}} \frac{1}{w_h \cdot w_v} e^{-8x^2/w_h^2} \cdot \text{rect}[y/w_v] \cdot \tau_a. \quad (2.6)$$

τ_a is the atmospheric transmission, and depends on range. τ_a can also be written $\tau_a = e^{-\sigma \cdot R}$, where σ is the damping coefficient of the atmosphere. x and y represent the horizontal and vertical axis respectively. w_h and w_v are the whole widths of the beam at the distance of the target. For small angles, the beam width can be approximated by the divergence, θ multiplied with the distance from the source R . In our model, w_h can be approximated this way

$$w_h = R \cdot \theta_h. \quad (2.7)$$

θ_h is the divergence of the beam in the horizontal direction. w_v can be found using

$$w_v = 2R \cdot \tan(\theta_v/2). \quad (2.8)$$

θ_v is the beam divergence in the vertical direction. w_v and θ_v use the $1/e^2$ definition of the limit of the whole width of the beam, while w_h and θ_h use FWHM, also of the whole length of the fan shape.

2.2.2 The target, a corner cube retroreflector

The target we will consider is a circular corner cube retroreflector. These are made up from three flat, reflecting surfaces at right angles to each other, and all the light that hits the reflecting area, will reflect back towards the source. Figure 2.8 illustrates how this works.

For distances so great that w_h is larger than the diameter of the reflector, d_{cc} the intensity of the reflected light will vary according to the light beam and the corner cube's lateral position in relation to each other. The maximum power that can be reflected is given by

$$P_{cc}^{max}(R) = \int_{-d_{cc}/2}^{d_{cc}/2} \int I_{target} \cdot dx dy \approx \frac{\pi}{4} \cdot \frac{P_t \cdot d_{cc} \cdot \tau_a}{w_v} \cdot \text{Erf} \left[\frac{\sqrt{2} \cdot d_{cc}}{w_h} \right]. \quad (2.9)$$

Because we here integrate over a square, and not a circle, the factor $\pi/4$ is included. The maximum effect that the detector can receive, P_r^{max} becomes

$$P_r^{max}(R) = P_{cc}^{max}(R) \frac{d_r^2 \cdot \rho_t}{4d_{cc}^2} = \frac{\pi}{16} \frac{P_t \cdot d_r^2 \cdot \tau_0 \cdot \tau_a^2 \cdot \rho_t}{2R \cdot \tan(\theta_v/2) \cdot d_{cc}} \text{Erf} \left[\frac{\sqrt{2} \cdot d_{cc}}{R \cdot \theta_h} \right] \quad (2.10)$$

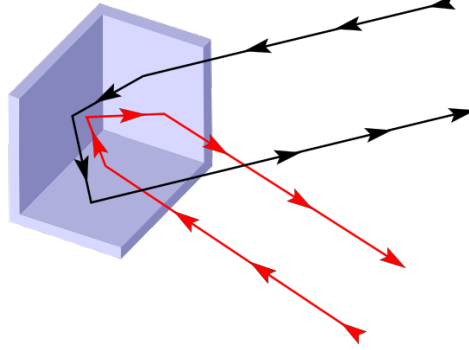


Figure 2.8: Illustration showing how a corner reflector works. The Illustrations shows two rays, red and black being reflected from different directions. Each ray is reflected three times.

d_r is the receiver diameter, τ_0 transmission of the receiver lens and ρ_t is the target reflectivity, a number of how much of the incident light that will be reflected. $Erf(x)$ is the error function, the result of integrating over the Gaussian distribution. If $x < 0.2$, the error function can be approximated by a linear function,

$$Erf(x) \approx \sqrt{\frac{2}{\pi}} \cdot x, \quad (2.11)$$

which simplifies the expression for maximum received power to

$$\begin{aligned} P_r^{max}(R) &= \frac{\pi}{16} \cdot \frac{P_t \cdot d_r^2 \cdot \tau_0 \cdot \tau_a^2 \cdot \rho_t}{2R \cdot \tan(\theta_v/2) \cdot d_{cc}} \cdot \sqrt{\frac{2}{\pi}} \left[\frac{\sqrt{2} \cdot d_{cc}}{R \cdot \theta_h} \right] \\ &= \frac{\sqrt{2\pi}}{16} \frac{P_t \cdot d_r^2 \cdot \tau_0 \cdot \tau_a^2 \cdot \rho_t}{R^2 \cdot \theta_h \cdot \tan(\theta_h/2)}. \end{aligned} \quad (2.12)$$

The range where this simplification can be used increases with a more narrow horizontal beam width, which has to be expressed in radian. For a corner cube with the diameter $d_{cc} = 60$ mm, and a beam divergence of 0.7 rad, this distance is $R = 600$ m.

The angle of incidence will also influence the reflected power. Normal angle will give the maximum reflected power. Anything else than that, will reduce the effective aperture area.

For large distances, the diffraction pattern of the corner cube becomes more predominant. The diffraction pattern of a circular aperture, is the Airy disk. The angle between the first minima, θ_{cc}^{diff} is

$$\theta_{cc}^{diff} = \frac{2.44 \cdot \lambda}{d_{cc}}. \quad (2.13)$$

For a corner cube with diameter $d_{cc} = 60$ mm, and using light with wavelength $\lambda = 1550$ nm, this diffraction becomes noticeable at approximately 2 km distance. Taking this into consideration when calculating the average illumination at the receiver, this expression for the area of the returned beam at the receiver, A_{rtn} can be used

$$A_{rtn} = \pi \left(d_{cc} + \frac{1.22\lambda R}{d_{cc}} \right)^2. \quad (2.14)$$

This can be further simplified. For $R \ll 2$ km we can use

$$A_{rtn} = \pi d_{cc}^2, \quad (2.15)$$

and for $R \gg 2$ km, we can use

$$A_{rtn} = \pi \left(\frac{1.22\lambda R}{d_{cc}} \right)^2. \quad (2.16)$$

The intensity of the light at the receiver will be

$$\begin{aligned} I_r(R) &= I(0, 0, 2R) \cdot \frac{d_{cc}^2}{\left(d_{cc} + \frac{1.22\lambda \cdot R}{d_{cc}} \right)^2} \\ &= \sqrt{\frac{2}{\pi}} \frac{2P_t \cdot \tau_a^2 \cdot \tau_0 \cdot \rho_t}{w_v(2R) \cdot w_h(2R)} \cdot \frac{1}{\left(1 + \frac{1.22\lambda \cdot R}{d_{cc}^2} \right)^2}. \end{aligned} \quad (2.17)$$

2.2.3 Receiver, detector and noise

The efficiency of a receiver is given by the optical transmission of the receiver lens, τ_0 and the quantum efficiency of the detector, η . τ_0 gives a number on how much of the received energy that reaches the detector. η tells us on average, how many of the photons that hit the detector will produce a photoelectron. Both the optical signal received at the detector and the electrical signal will contain noise. Sensitivity for a sensor is determined to a large extent by the noise level in the detector output.

One source of noise comes from the fact that photons occur independent of each other and the discretization that happens in the detector. This is the photon noise. During the detector integration time, Δt the number of photons that hit the detector and are transformed into electrons is random. On average, the number will be the expected value. Using a detector where η is less than 1, will strengthen this effect.

A laser beam that has been reflected off of a target surface will cause speckle noise in the detector. The noise arise from the interference of many independent, coherent radiators. The noise that is added is proportional with the square of the incident power. For highly coherent light, this noise becomes more dominant.

Thermal noise is generated in the detector itself. All things that have a temperature above 0 K will emit photons. The noise caused by these photons is commonly called dark current. It is the current that can be measured when there is no light present.

Background noise is generated from light that is collected by the detector, but does not come from the laser source originally. This is typically sunlight. To reduce the amount of unwanted background noise, one can use a bandpass filter that will stop most light with other than a specific wavelength to reach the detector. In practice, the detection of a signal is often limited by the background noise.[8]

2.3 Signal to noise ratio

The signal to noise ratio, SNR in short, is basically the ratio between the peak value of the signal to the RMS value of the noise.

$$SNR = \frac{Signal_{peak}}{Noise_{rms}}. \quad (2.18)$$

SNR is unitless, and can be used for any kind of signal, not only electrical.

When a detection system must decide whether the target is present or not, four things can happen:

1. A signal is detected when there is a signal present, a **true detection**.
2. There is a signal present, but it is not detected.
3. There is no signal present, but there is still a detection, a **false detection**
4. There is no signal present and no signal is detected.

To optimise the detection system, the amount of wrong decisions must be reduced, and the probability of detection must be maximised. To achieve this, the SNR must be larger than some threshold value, which will depend on the performance of the system.[5] One way to determine this value, SNR_{min} will be discussed below, this method assumes that both the signal and the noise have gaussian probability density function.

2.3.1 Statistics of the sensor output signal

In order to detect the presence of a target, there must be a difference in the output signal voltage coming from the sensor when there is a target present and when there is not. Usually, the voltage, v coming from the sensor is compared to some threshold value, v_{th} and one of two things can happen:

- if $v > v_{th} \rightarrow$ presence of target
- if $v < v_{th} \rightarrow$ absence of target

The challenge now is, what values should be given to v_{th} and SNR in order to satisfy the desired probability of detection, P_d and probability of wrongful detection, also known as the probability of false alarm, PFA. The statistical characteristics of the output signals will help with this, specifically their probability density function, PDF.

When there is no target present, the output voltage will be characterised by the noise pdf, $p_n(v)$. For simplicity, assume that its mean value is 0. When the target is present, the PDF of the output voltage changes to $p_{s+n}(v)$. Its average value, corresponds to that of the signal flux that is incident upon the detector, v_s . The RMS value of the PDFs are $\sigma_{v,n}$, when obtained in absence of a target, and $\sigma_{v,s+n}$ when obtained in the presence of a target.

Figure 2.9 illustrates the noise PDF and three PDF of a signal when the target is present. The three signals are different in strength, one can understand that determining if a target is present or not, becomes easier the further apart the curves of the signal and the noise are. The larger the ratios $v_s/\sigma_{v,n}$ $v_s/\sigma_{v,s+n}$ are, the better the performance of the sensor.

2.3.2 Probability of detection and false alarm

The probability to rightfully detect when a target is present is the probability that the output voltage signal from the sensor is above the threshold value when the target is present. This probability is found by integrating $p_{s+n}(v)$ from v_{th} and upwards

$$P_d = \int_{v_{th}}^{\infty} P_{s+n}(v)dv. \quad (2.19)$$

Likewise, the probability of a false alarm, to wrongfully detect a target when there is no target present, is the probability that the output voltage signal from the sensor is above v_{th} even if there is no target present

$$P_{FA} = \int_{v_{th}}^{\infty} P_n(v)dv. \quad (2.20)$$

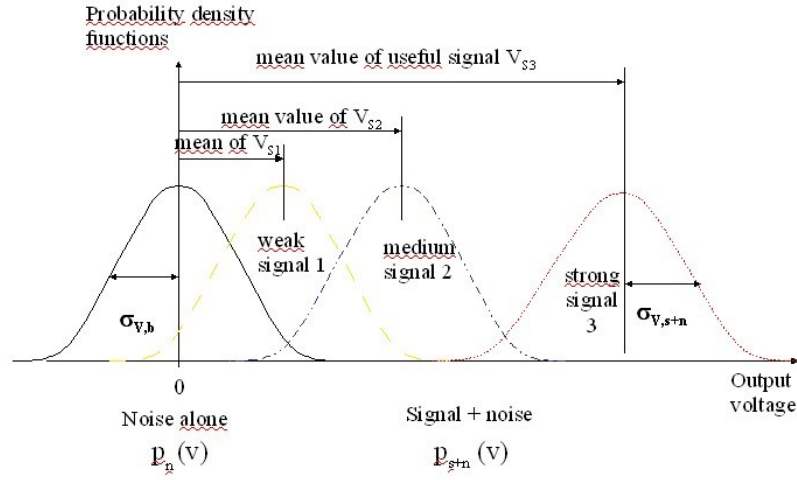


Figure 2.9: PDF of three signals of different strengths and noise PDF. [5]

As it is assumed that the PDFs of the noise and signal are gaussian, the PDF of the noise is

$$p_n(v) = \frac{1}{\sqrt{2\pi\sigma_{v,n}^2}} e^{-\frac{v^2}{2\sigma_{v,n}^2}}, \quad (2.21)$$

and the PDF of the signal is

$$p_s(v) = \frac{1}{\sqrt{2\pi\sigma_{v,n}^2}} e^{-\frac{(v-v_s)^2}{2\sigma_{v,n}^2}}. \quad (2.22)$$

This gives the probability of detection,

$$P_d = \frac{1}{\sqrt{2\pi\sigma_{v,n}^2}} \int_{v_{th}}^{\infty} \exp\left(-\frac{(v-v_s)^2}{2\sigma_{v,s+n}^2}\right) dv \quad (2.23)$$

and the probability of false alarm

$$P_{FA} = \frac{1}{\sqrt{2\pi\sigma_{v,n}^2}} \int_{v_{th}}^{\infty} \exp\left(-\frac{v^2}{2\sigma_{v,n}^2}\right) dv. \quad (2.24)$$

The probability of false alarm decrease rapidly the larger the ratio $v_{th}/\sigma_{v,n}$ becomes.

2.3.3 Determining the minimum value of SNR

In order to find the minimal SNR, the inverse function of the PDF is needed. The cumulative distribution function of the standard normal distribution is

$$f(x) = \frac{1}{\sqrt{2\pi}} \int_{-\infty}^x e^{-\frac{t^2}{2}} dt. \quad (2.25)$$

$f(x) = y$ has an inverse function $x = g(y)$. This also counts for the functions for PFA and P_d above.

$$P_{FA} = f\left(\frac{-v_{th}}{\sigma_{v,n}}\right) \quad (2.26)$$

gives

$$\frac{v_{th}}{\sigma_{v,n}} = -g(P_{FA}), \quad (2.27)$$

which means that by choosing a desired PFA, the $v_{th}/\sigma_{v,n}$ ratio can be determined. The function for probability of detection is

$$P_d = f\left(\frac{v_s - v_{th}}{\sigma_{v,s+n}}\right), \quad (2.28)$$

and gives the inverse function

$$\frac{(v_s - v_{th})}{\sigma_{v,s+n}} = -g(P_d). \quad (2.29)$$

To simplify further, it is assumed that the system is stationary and weak enough that its presence does not influence the noise level significantly,

$$\sigma_{v,s+n} \approx \sigma_{v,n}. \quad (2.30)$$

Using this, equation 2.27 and 2.29 can be combined

$$\frac{v_{th}}{\sigma_{v,n}} = g(P_d) - g(P_{FA}). \quad (2.31)$$

This means that the minimum signal to noise ratio to satisfy the probability of detection and probability of false alarm is

$$SNR_{min} = g(P_d) - g(P_{FA}). \quad (2.32)$$

The table below gives values for $g(y)$ for some arguments, y .

As an example, if the desired probability of detection is $P_d = 95\%$ and probability of false alarm is $P_{FA} = 10^{-3}$, the minimum signal to noise ratio becomes $SNR_{min} = 1.64 - (-3.09) = 4.73$

Table 2.2: A selection of arguments and their corresponding values for $g(y)$ [5].

y	$g(y)$	y	$g(y)$	y	$g(y)$	y	$g(y)$
10^{-12}	-7,03	$2 \cdot 10^{-3}$	-2,87	0,6	0,25	$1 \cdot 10^{-4}$	3,71
10^{-11}	-6,7	$5 \cdot 10^{-3}$	-2,57	0,7	0,52	$1 \cdot 10^{-5}$	4,26
10^{-10}	-6,36	10^{-2}	-2,32	0,8	0,84	$1 \cdot 10^{-6}$	4,75
10^{-9}	-5,99	$2 \cdot 10^{-2}$	-2,05	0,9	1,28	$1 \cdot 10^{-7}$	5,19
10^{-8}	-5,61	$5 \cdot 10^{-2}$	-1,64	0,95	1,64	$1 \cdot 10^{-8}$	5,61
10^{-7}	-5,19	10^{-1}	-1,28	0,98	2,05	$1 \cdot 10^{-9}$	5,99
10^{-6}	-4,75	$2 \cdot 10^{-1}$	-0,84	0,99	2,32	$1 \cdot 10^{-10}$	6,36
10^{-5}	-4,26	$3 \cdot 10^{-1}$	-0,52	1	2,57	$1 \cdot 10^{-11}$	6,7
10^{-4}	-3,71	$4 \cdot 10^{-1}$	-0,25	1	2,87	$1 \cdot 10^{-12}$	7,03
10^{-3}	-3,09	$5 \cdot 10^{-1}$	0	1	3,09		

2.4 Laser safety

Eye safety when dealing with lasers was discussed in [1], but a brief recap of the most important points will be repeated here. There are four main classes for laser safety, separated by the lasers ability to hurt the eye or skin when in use. MPE is the highest power or energy density that is considered safe. The MPE limits differ across wavelengths. The lowest MPE is for wavelengths between 400 and 1400 nm, and includes the wavelengths for visible light. At these wavelengths, the eye is most susceptible for retinal damage. Figure 2.10 gives an overview of the MPEs versus wavelength for different exposure times (pulse durations). Which MPE to use for a pulsed laser is found by using the most limiting of three rules:

1. The exposure limit for a single pulse
2. The exposure limit for average power, which corresponds to the MPE of a pulse of duration T_{max}
3. No pulse should exceed the MPE for a single pulse multiplied with a correction factor C_5

For wavelengths shorter than 400 nm or longer than 1 400 nm, the MPE is determined by either number 1 or 2.

The nominal ocular hazard distance is the distance from the output aperture at which the radiant exposure is below the MPE,

$$NOHD = \sqrt{\left(\frac{4P_{avg}}{\pi \cdot MPE} - w_{0,1/e}^2\right)} \cdot \frac{1}{\theta_{1/e}}. \quad (2.33)$$

$w_{0,1/e}$ is the $1/e$ -diameter of the beam at the beam waist and $\theta_{1/e}$ is the full angle divergence at $1/e$.

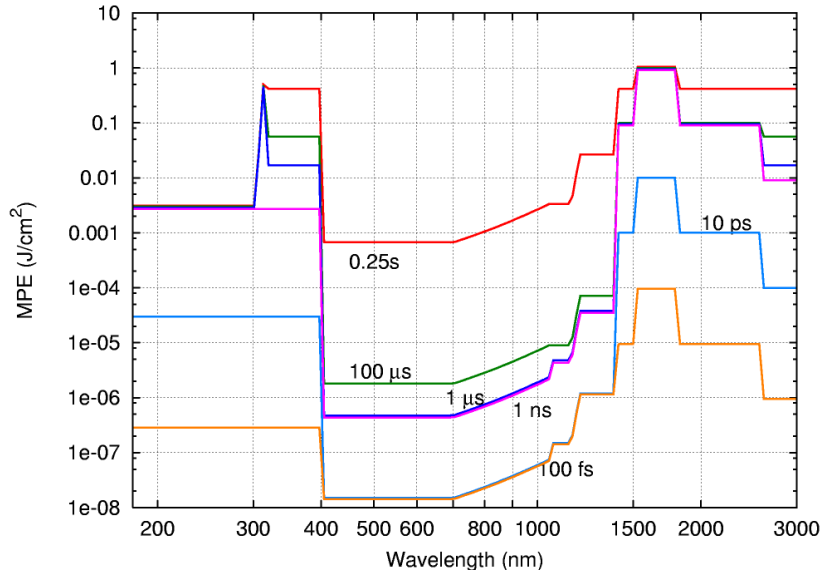


Figure 2.10: MPE versus wavelength for different exposure times (pulse durations) [9].

When calculating exposure values, a circular aperture is used. In the spectral range between 1 400 nm and 10^5 nm, an aperture with $d_a = 1$ mm diameter is used to evaluate the hazard of individual pulses. Exposures greater than 10 s are evaluated using an aperture with $d_A = 3.5$ mm diameter. When the beam width is larger than d_A , the total power transmitted through the circular aperture can be approximated by

$$\frac{\Phi_d}{\Phi_0} = \frac{\pi d_A \cdot \text{Erf}[\sqrt{2} \cdot d_A/w_h]}{4w_v}. \quad (2.34)$$

To find the average exposure over this aperture, equation 2.34 is multiplied with Φ_0 and divided by the aperture area. Φ_0 is given by

$$\Phi_0 = K_{sys} \cdot Pt \cdot w_h \cdot w_v \cdot \sqrt{\pi/8}. \quad (2.35)$$

The aperture area is $7.85 \cdot 10^{-3}$ cm² for single pulse, and $9.62 \cdot 10^{-2}$ cm² for long exposures.

2.5 Figure of merit

When comparing possible systems against each other, there needs to be some criteria that emphasise the parameters that sets the alternatives apart from each other. Figure of merit, FOM gives a number to different alternatives so that they can be

compared to each other. For systems that use different combinations of lasers and detectors, FOM must encompass central qualities for both lasers and detectors. In this application, the lasers will be pulsed. The peak power of the pulse is important in deciding the range of the system. For detectors, the strength of the electrical signal initiated by the incoming light is an important factor. Another option is to consider the noise generated in the detector and use the noise equivalent power (NEP). It was chosen to use the pulse peak power, P_t , $G = TI\ Gain \cdot R_0 \cdot M$ and a calculated NEP as parameters for the FOM divided by the same factors for SpotTrack to get an estimate of the improvement compared to that

$$FOM = \frac{P_t^x \cdot G^x}{P_t^{ST} \cdot G^{ST}} \cdot \frac{NEP_{calc}^{ST}}{NEP_{calc}^x}. \quad (2.36)$$

x represents the system combination of laser and detector. TI Gain is the transimpedance gain, R_0 is the responsivity of the detector and M is a factor for manual gain. For SpotTrack, FOM will of course be equal to 1, and

$$\frac{P_t^{ST} \cdot G^{ST}}{NEP_{calc}^{ST}} = 7.75 \cdot 10^{-4} \text{ V}.$$

Theoretical calculations

3.1 Range

Section 2.2 presented an expression for the power that is reflected onto a detector from a laser beam via a target, equation 2.10. Here, this will be used together with information about three proposed systems to find an estimation of how far away a target can be detected. Information about the systems can be found in the tables below.

The systems are based on a laser diode (LD) from the 1550 HI-series from Laser Components [10] and a 1550 nm KULT2 fiber laser (FL) from Keopsys [11]. The detectors used are a PIN photodiode [12] and an avalanche photodiode (APD) [13].

Table 3.1 presents the two lasers. For both of them, the *prf* was set manually and the average power was measured, from which E_p and P_t was calculated using a simple excel sheet[7]. The horizontal beam divergence, $\theta_{h,FWHM}$ is also a measured property, as it is in combination with an aspheric lens. It is also worth noting that the measured peak power for both the lasers is considerably lower than what is stated in the data sheet. The average power of the LD was measured to be 0.4 mW, giving a peak power of 1 W, the data sheet [10] states that peak power at maximum current will be 30 W. The average power of the FL was measured to be 295 mW, which gives a P_t of 2000 W. In the datasheet, P_t should be 4000 W. Entries marked with an '*' in table 3.1 come from the laser data sheets [10] and [11], the rest are either measured or calculated based on the measurements.

The target presented in table 3.2 is a corner cube retroreflector with a circular aperture as described in section 2.2.2.

The receiver lens has a diameter of 48 mm and collects and concentrates the light onto the detector surface.

The characteristics of the two detectors are presented in table 3.4. They are

Table 3.1: Characteristics for two kinds of lasers with 1550 nm wavelength, a diode laser (LD) and a fiber laser (FL).

Laser type	FL	LD	Unit
pulse repetition frequency, prf	21	3.3	kHz
average power P_{avg}	294	0.04 ¹	mW
Pulse energy, E_p	14	0.012	μ J
Pulse width, t_w	7	14.3	ns
Peak power, P_t	2000	0.84	W
Datasheet peak power, $P_{t,ds}^*$	4000	30	W
Data sheet pulse width at peak power, $t_{w,ds}^*$	7	150	ns
FWHM Beam div. vert. $\theta_{v,FWHM}^*$	12	12	deg
FWHM Beam div. hor. $\theta_{h,FWHM}$	0.818	2.85	mrاد

Table 3.2: The target, a corner cube retroreflector.

Target type	Circular corner cube	Unit
Diameter, d_{cc}	60	mm
Traget area, A_{cc}	$2.8 \cdot 10^{-3}$	m ²
Reflectivity[7], $refl$	0.8	

both InGaAs photodiodes [12][13]. Entries marked with and '*' are from the data sheets, the rest are either calculated or based on measurements.

Table 3.5 presents three combinations for the system. K_{sys} sums up all the constants in equation 2.10. Probability of false alarm, and the false alarm rate are chosen to have a small error rate, and at the same time to have a fair amount of true detections. To fulfil these requirements, the SNR must be 4.6 or higher. Multiplied with the NEP, this gives the lowest detectable signal power on the detector. Based on these values, the figures below give illustrations of all three combinations.

SNR_{min} was found using the method in chapter 2.3. Figure 3.1 shows the expected power on the detector when the FL and APD are used. The detection threshold is included as well. The range is shown for five different weather conditions. Very clear weather corresponds to visibility of 23.5 km or more. 5 km or more visibility are clear weather conditions and so on. Figure 3.2 illustrates the voltage output the detector will have for the different weather conditions and ranges. The APD has an adjustable gain between $M = 4$ and $M = 20$, and so the detector output is shown for both those gains as well. Pink colours represent $M = 4$ and blue and green colours represent $M = 20$. The maximum voltage output from the detector is 2 V.

¹measured at 10 kHz

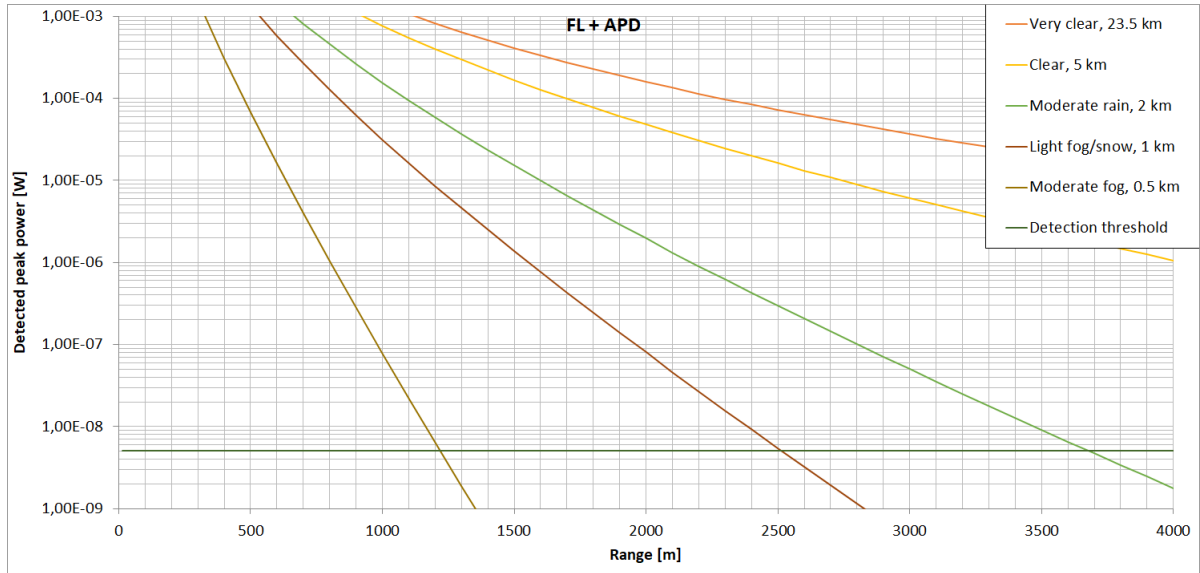


Figure 3.1: Power reflected onto the detector for the FL and APD combination for five different visibilities.

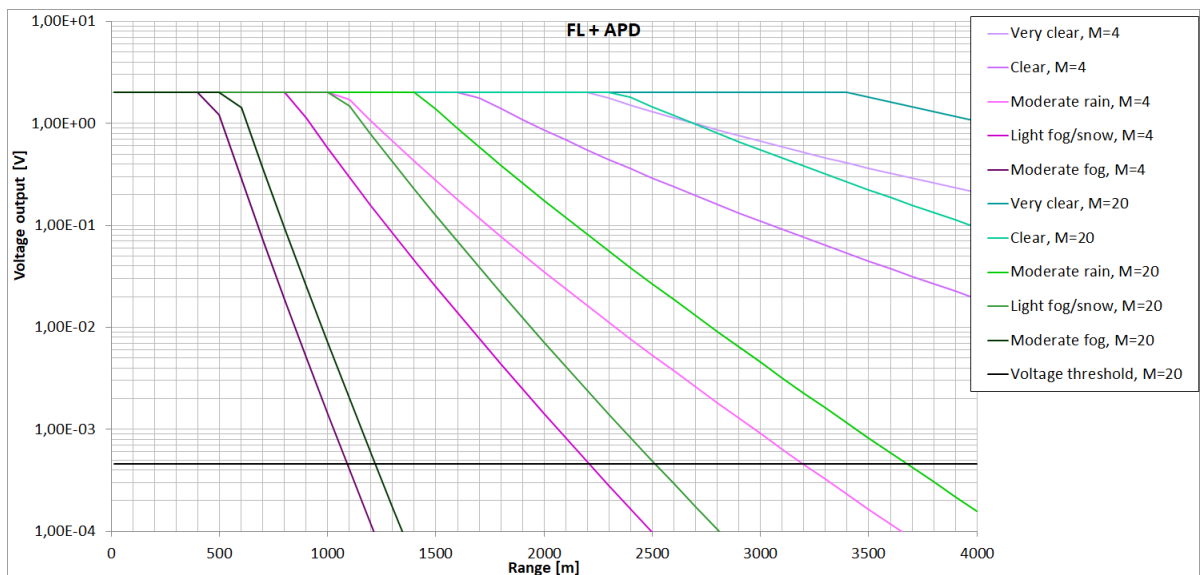


Figure 3.2: Voltage output for the FL and APD combination for five different visibilities. Pink colours represent detector gain of 4, and green/blue colours represent a gain of 20.

Table 3.3: Receiver lens characteristics, identical for all three laser systems.

Parameter	Value	Unit
Diameter, d_r	48	mm
Area, A_r	18.10	cm ²
Transmission, τ_0	0.6	

Table 3.4: Detectors with amplifiers

Detector type	PIN	APD	Unit
* Responsivity, R_0	1.04	18	A/W
* Gain, M	1	20	
* Detector bandwidth	150	400	MHz
* NEP (λ_p)	12	0.45	pW/ $\sqrt{\text{Hz}}$
* Max. input power		1	mW
* Max. output current	100		mA
* Max. output voltage (50 Ω)	5	2	V
* TI Gain	5000	5000	V/A
Input impedance, R_L	6000	6000	Ω
Current noise	3	1	pA/ $\sqrt{\text{Hz}}$
* Signal Bandwidth	150	400	MHz
* Noise bandwidth	150	100	MHz
Voltage noise	0.82	0	nV/ $\sqrt{\text{Hz}}$

Table 3.5: The three combinations and their properties.

System	FL+APD	FL+PIN	LD+APD	Unit
K_{sys}	34.4	34.4	$1.72 \cdot 10^{-2}$	
Prob. of detection, P_d	0.95	0.95	0.95	
prob. of false alarm, PFA	0.001	0.001	0.001	
NEP_{calc}	$1,11 \cdot 10^{-9}$	$3,53 \cdot 10^{-8}$	$1,11 \cdot 10^{-9}$	W
$\text{SNR}_{\text{min.}} = 4.7$	$5.2 \cdot 10^{-9}$	$1.66 \cdot 10^{-7}$	$5.2 \cdot 10^{-9}$	W

Figure 3.3 shows the expected power on the detector for the LD and APD combination using the parameters given in tables 3.1 and 3.4. Figure 3.4 shows the expected voltage output for the same combination and the same five visibilities. Maximum voltage output from the detector is 2 V.

Figure 3.5 shows the expected power on the detector for the FL and pin combination at different weather conditions and ranges. Figure 3.6 shows the expected voltage output of the detector under the same conditions. The maximum voltage output of the pin photodetector is 5 V.

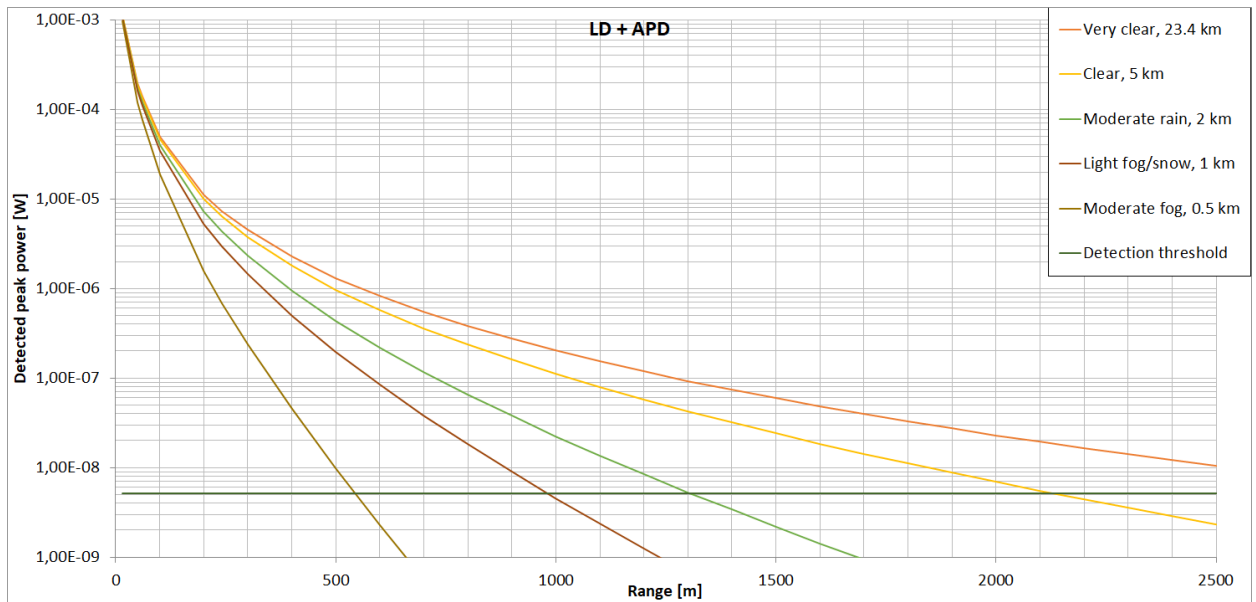


Figure 3.3: Power reflected onto the detector for the LD and APD combination for five different visibilities.

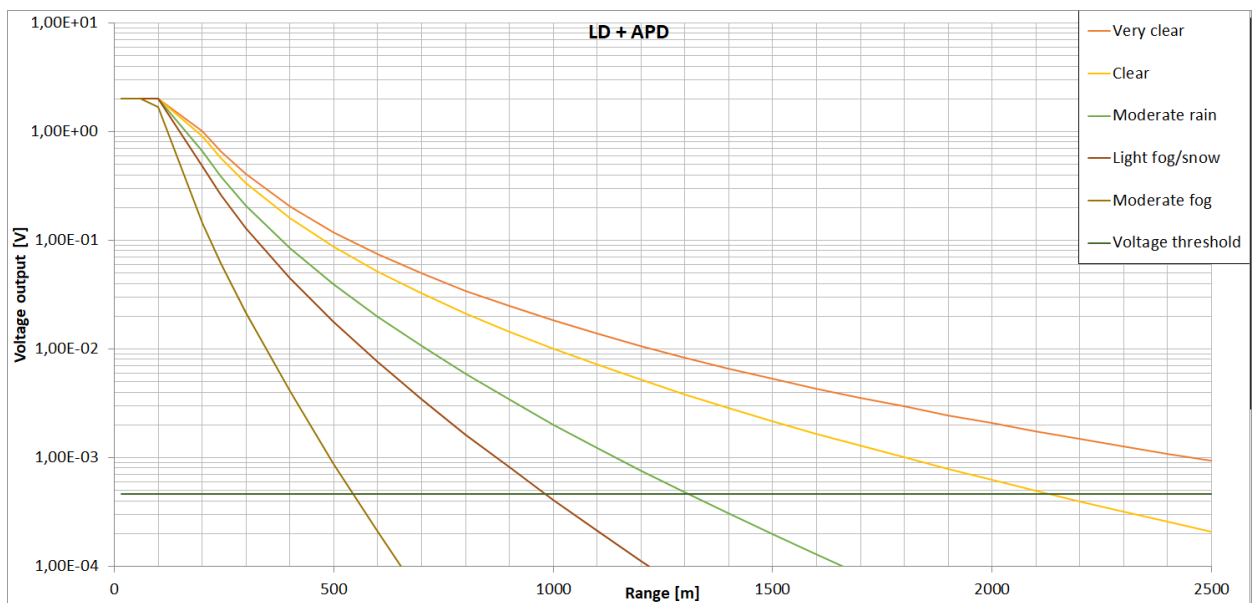


Figure 3.4: Voltage output for the LD and APD combination for five different visibilities.

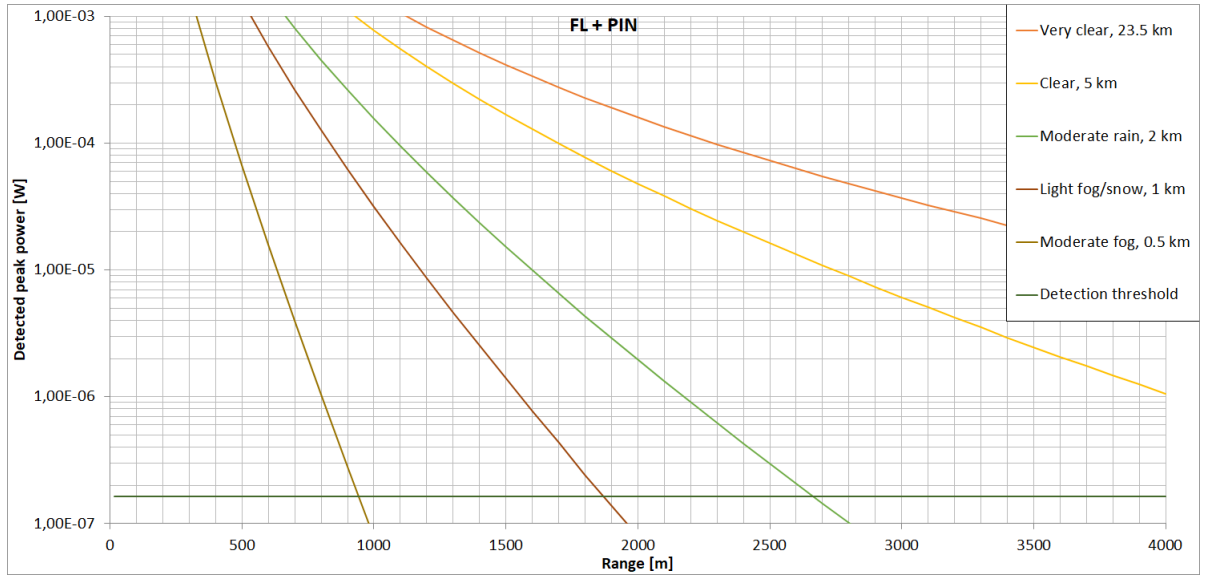


Figure 3.5: Power reflected onto the detector for the FL and pin combination for five different visibilities.

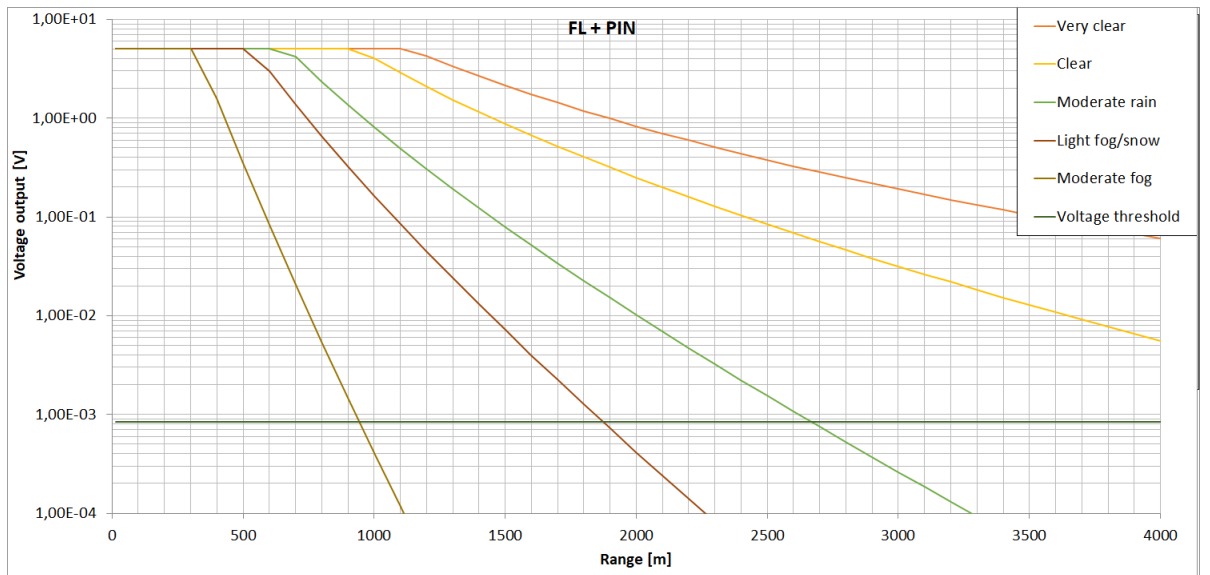


Figure 3.6: Voltage output for the FL and pin combination for five different visibilities.

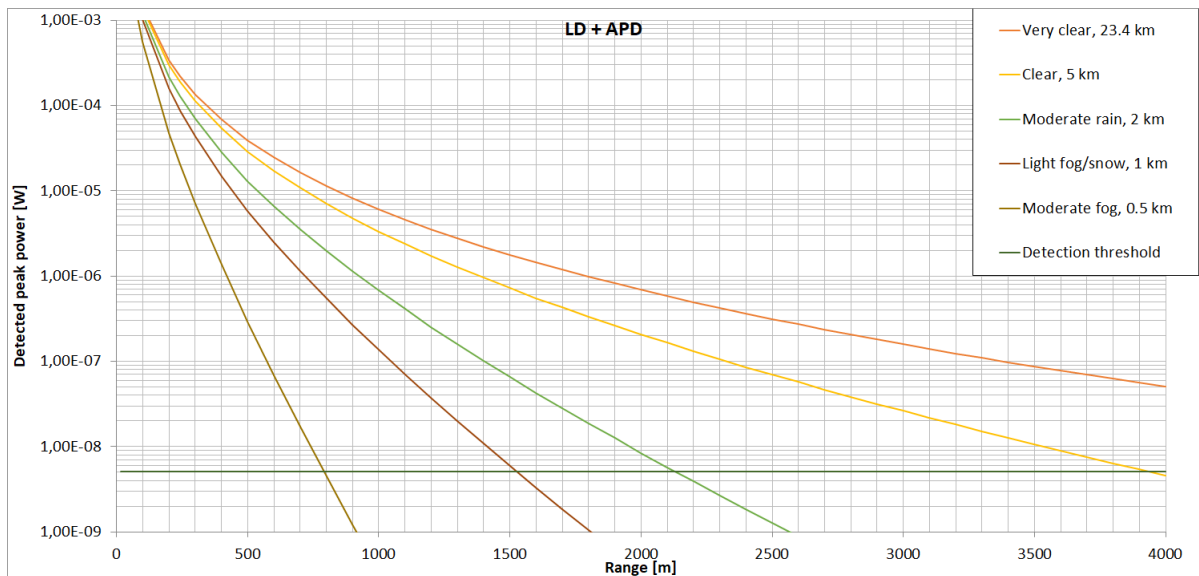


Figure 3.7: Power reflected onto the detector for the LD and APD combination if P_t is 30 W, under five different weather conditions. Detection threshold included.

The last two figures, figure 3.7 and 3.8 are the calculated power on and output voltage from the detector for the combination of LD and APD if the peak pulse power, P_t is 30 W as is stated in the data sheet. [10]

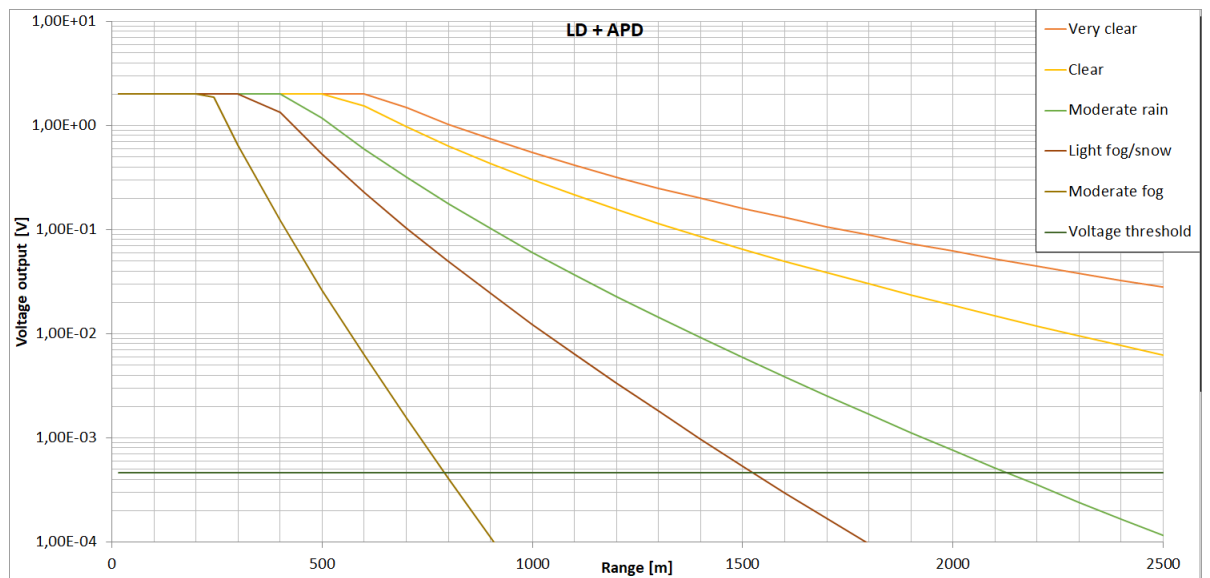


Figure 3.8: Voltage output from the the detector in the LD and APD combination if P_t is 30 W and $M = 20$, under five different weather conditions.

3.2 Results of safety calculations

For both the LD and the FL, the limiting factor is the average power, rule nr. 2 in section 2.4. For single pulses, the MPE = 10^4 J/m². The MPE of the average power P_{avg} is 1 000 W/m².

By using the information about the lasers found in table 3.1, the safe distance, NOHD was found for situations when the lasers are standing still, sending out maximum peak power and without any protective housing. For the laser diode, the safe distance is

$$NOHD_{LD} = 5 \text{ cm.} \quad (3.1)$$

For the fiber laser, the safe distance is

$$NOHD_{FL} = 2.1 \text{ m.} \quad (3.2)$$

The NOHD will be lowered to 1.1 m if the average power is reduced to 300 mW at the same *prf*. It will be further lowered to 0.6 m when $P_{avg} = 200$ mW.

3.3 FOM and costs calculations

Section 2.5 gives an expression to determine the figure of merit for the different combinations of laser and detector. Using the information given in tables in section 3.1, we can find FOM for the different combinations. Table 3.1 states that

- $P_{t,ds}^{LD} = 30$ W
- $P_{t,ds}^{FL} = 4000$ W

From table 3.4 we know that

- TI Gain^{PIN} = $5 \cdot 10^3$ V/A and $R_0^{PIN} = 1.04$ A/W
- TI Gain^{APD} = $5 \cdot 10^3$ V/A and $R_0^{APD} = 9 \cdot 10^4$ A/W

And table 3.5 tells us that

- $NEP_{calc}^{PIN} = 3.53 \cdot 10^{-8}$
- $NEP_{calc}^{APD} = 1.11 \cdot 10^{-9}$

Using equation 2.36, we can compare it to the Spot Track and get a number for the FOM.

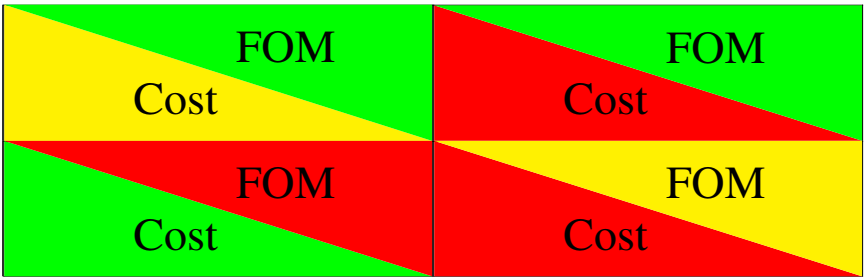
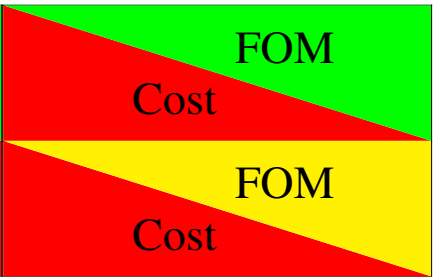
- $FOM^{LD+PIN} = 0.05$
- $FOM^{FL+PIN} = 7$
- $FOM^{LD+APD} = 30$
- $FOM^{FL+APD} = 4021$

To get a cost estimate, price was requested for APDs, PIN detectors, FL and LD price per piece for a batch of 50 pieces. Based on the offers, the average price per piece for LD, PIN etc. was calculated. The average price for each combination was then compared to the price of laser and detector in Spot Track. The price of these pieces were given per piece for a batch of 100 pieces. The increase in costs for the different combinations are:

- $Cost^{LD+PIN} \approx 2xST$
- $Cost^{LD+APD} \approx 5xST$
- $Cost^{FL+PIN} \approx 15xST$
- $Cost^{FL+APD} \approx 18xST$

Table 3.6 below is a chart covering the FOM and the costs of the different combinations. for FOM, **red** represents a FOM of less than 5, **yellow** between 5 and 20 and **green** above 20. **green** cost block means less than 5xST, **yellow** between 5 and 10xST and **red** means more than 10xST.

Table 3.6: The costs and the FOM for four different combinations.

	LD	FL
APD	 <p>FOM Cost</p>	 <p>FOM Cost</p>
PIN	 <p>FOM Cost</p>	 <p>FOM Cost</p>

Experiment

4.1 experimental work



Figure 4.1: The fiber laser and APD mounted on the prototype.

The setup to test the theoretical calculations is shown in figure 4.1. It includes the prototype on top of a rotating stage, an oscilloscope, a pulse generator, a variable power source to the laser and a computer to control the rotating stage. On

the prototype, the laser can be changed by using the different mounts for the different kind of lasers. The fiber laser was connected via the collimator. The diode laser was fastened using screws. The two detectors were similar in size and shape, and was fastened to the prototype using the same kind of mount. A band pass filter was put on top of the detectors to reduce the amount of background noise. A closer view of this is shown in figures 4.2 and 4.3. Figure 4.4 shows the top of the prototype from the front. A small screen of cardboard has also been put up to limit noise. The view from the prototype is seen in figure 4.5. The position of the retroreflector, 240 m away, is marked by a red box.

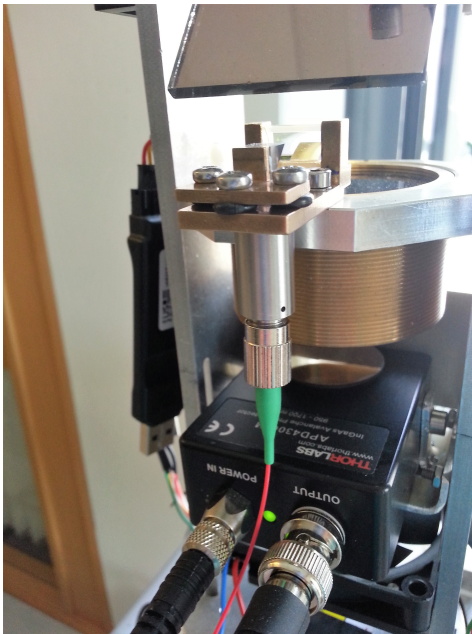


Figure 4.2: The fiber laser and APD mounted on the prototype.



Figure 4.3: The diode laser and APD mounted on the prototype.

The detector was connected to an oscilloscope. Also connected to it, was the trigger pulse of the laser. The laser was connected to a power source as well. The laser diode had a constant 5 V input, but the voltage to the fiber laser could be adjusted using a wheel. This influenced the laser output power.

The average output power of the FL, P_{avg} versus input voltage was measured using the thermal power sensor S302C from ThorLabs, connected to the laser via the collimator. The output voltage was connected to a voltmeter. After the voltage had been adjusted, the power was measured after three minutes. This was done for every 0.1 V up to 1 V. The result can be seen in table 4.1 and figure 4.6.

The tests themselves were all carried out in clear weather. The target, a retroreflector was placed on top of a pole 240 meters away. The laser beam would then

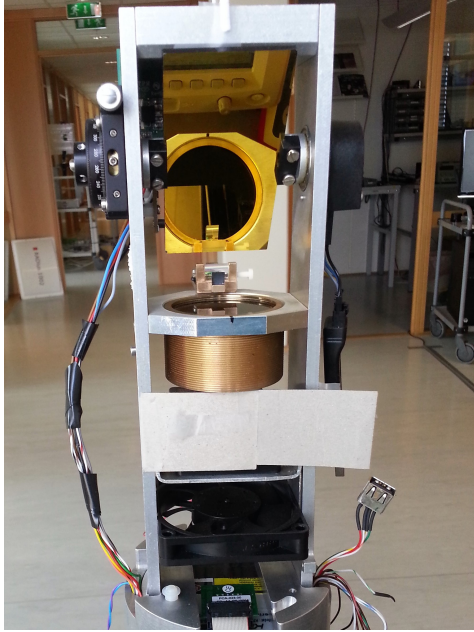


Figure 4.4: Upper front side of the prototype

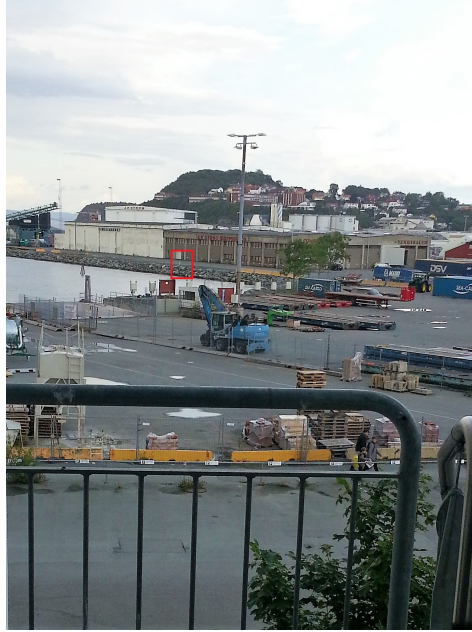


Figure 4.5: The view from the prototype testing. The location of the reflector is marked by a red rectangle.

Table 4.1: Input power to the FL versus the average output power, P_{avg} emitted by the fiber laser.

Voltage in [V]	P_{avg} [mW]
0.3	1.671
0.4	30.13
0.45	47.8
0.5	69.3
0.6	109.8
0.7	157
0.8	197.4
0.85	214.3
0.9	235.6
1	283.3
1.0279	294

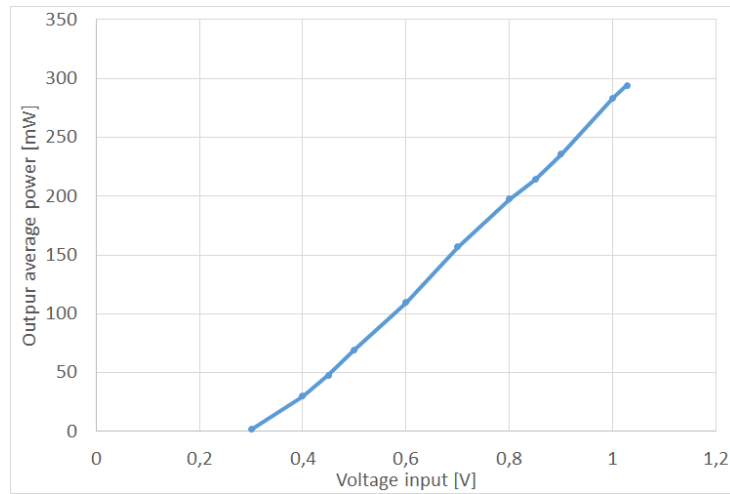


Figure 4.6: Input power to the FL versus the average output power, P_{avg} emitted by the fiber laser.

be aimed at it and the reflected beam would be measured using the oscilloscope that was connected to the detector. The oscilloscope was connected to both the trigger pulse and the detector, but because of some time delay in the laser, it could not be used as the starting time to find the distance to the target. This starting point was found by holding a white sheet of paper right in front of the laser, giving a peak that the oscilloscope cursor could be set at. Figure 4.7 shows an example of this pulse, where the green is the trigger pulse, and the yellow comes from the detector. Figure 4.8 shows the returned pulse from the target at 240 m distance together with the trigger pulse. The distance to the target was mainly used to compare the ranging equation predictions and experimental results, but also to control that the reflection came from the retroreflector and not something else, as there were many things that could give a strong reflection. Cars passing by and metallic fences being two common examples.

Because the target was so close, the detectors would saturate if the FL was used at full power. The input voltage were therefore lowered to an amount where light reflected from a white paper sheet right in front of the laser would not make the detector saturate. This happened at 0.3 V input, 1,67 mW average output power. By adjusting the value for average output power, P_{avg} in section 3.1 and therefore P_t in equation 2.10, the reflected power on the receiver P_r^{max} in equation 2.10 will be altered accordingly.

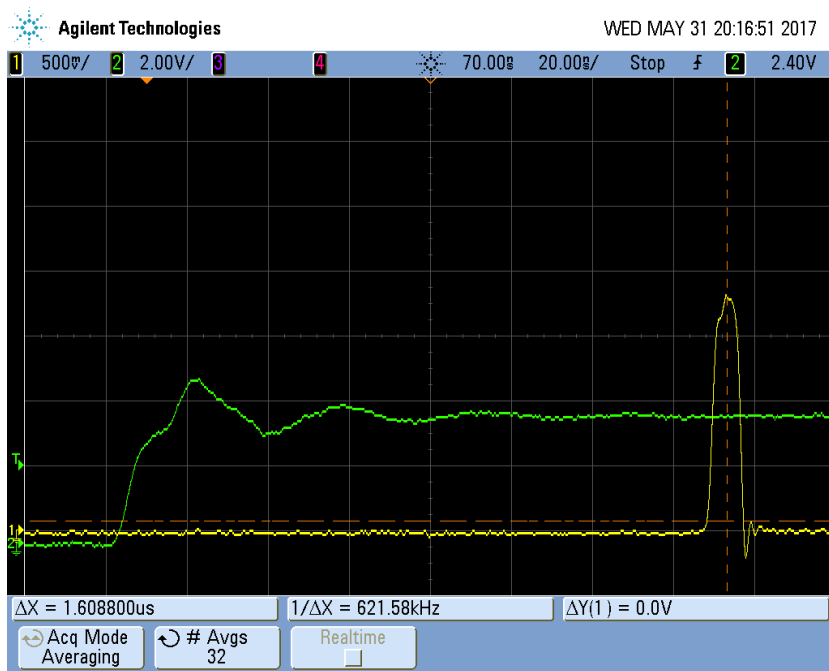


Figure 4.7: Trigger pulse and pulse from very close reflection.

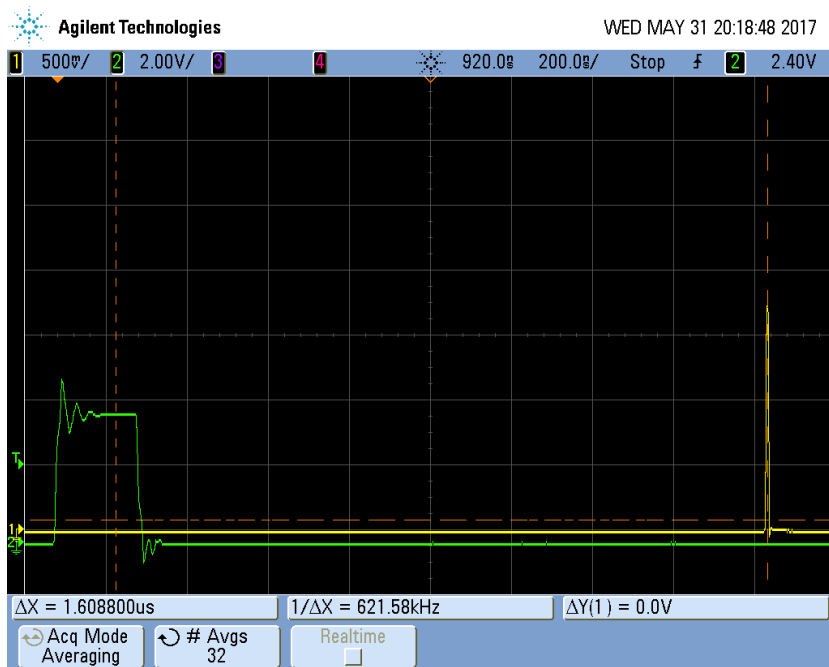


Figure 4.8: Trigger pulse and returned pulse from target at 240 m distance.

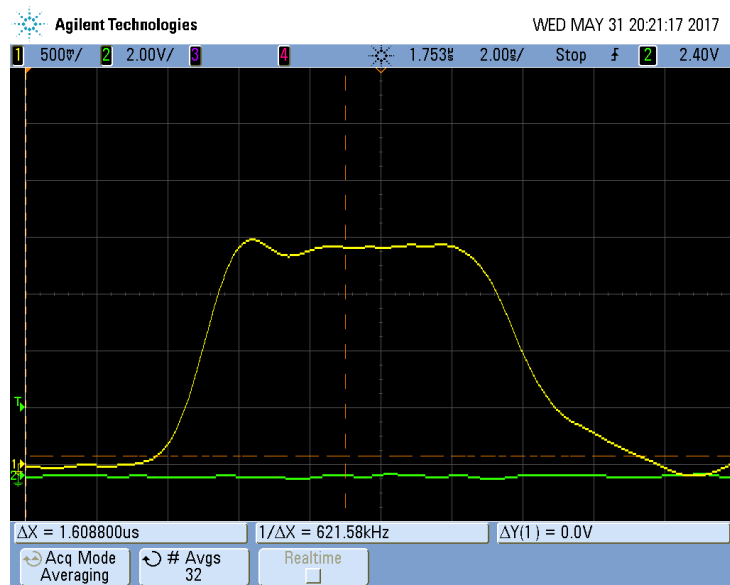


Figure 4.9: Even though the signal on average is not enough to saturate the APD, some of them do.

4.2 Experimental results

Starting out with the results for the FL and APD combination, equation 2.10 says that the detector will saturate if the average output power P_{avg} is 1.67 and the gain in the detector is $M = 4$. According to equation 2.10, the detector will no longer saturate at a target distance of between 3 and 400 meters. The experiment shows that many pulses are high enough to saturate the detector, as shown in figure 4.9, but on average, it is not. When averaging over 32 pulses, the returned pulse peak power gives the output voltage 1.14 V. This is shown in figure 4.10.

Figure 4.11 shows the reflected pulse from the combination of FL and pin detector. Here too, P_{avg} from the laser is 1.67 mW. This should give an voltage from the detector of 1.4 V. The returned peak voltage varies over time. at one point, the peak voltage from the detector is 2.7 V as shown in figure 4.11, but minutes later it has risen to 4 V without any noticeable change in the weather conditions. See figure 4.12.

The combination LD and APD should give 1 V output when $M = 20$ at the APD even when the average output power from the laser is as low as 0.04 mW. However, the experimental results did not show any reflected pulse. And the pulse returned when holding up a white sheet of paper is also well below 1 V. At the highest it is 240 mV. See figure 4.13. This suggest that the laser beam was not properly collimated at the time of these tests. This will be discussed further in chapter 5.

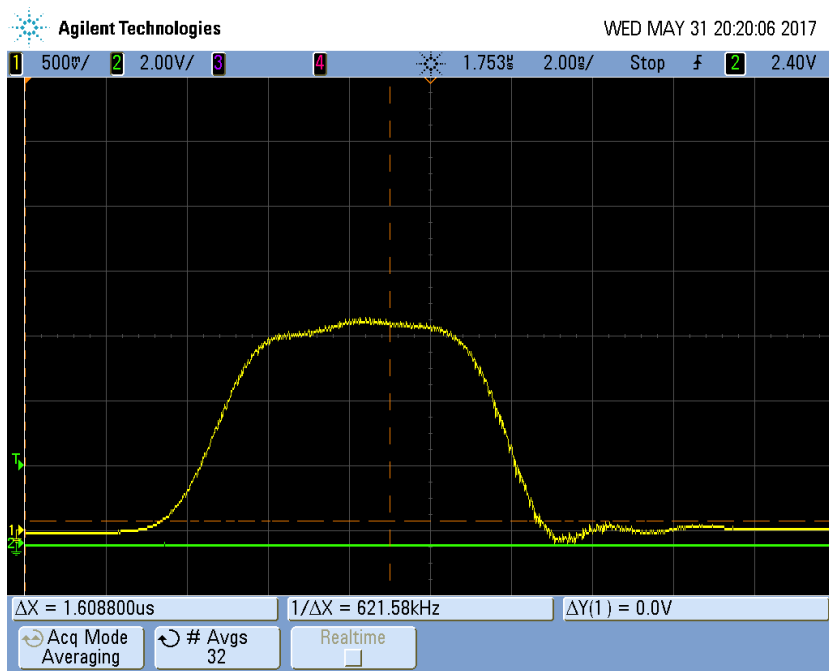


Figure 4.10: Output signal from APD when averaged.

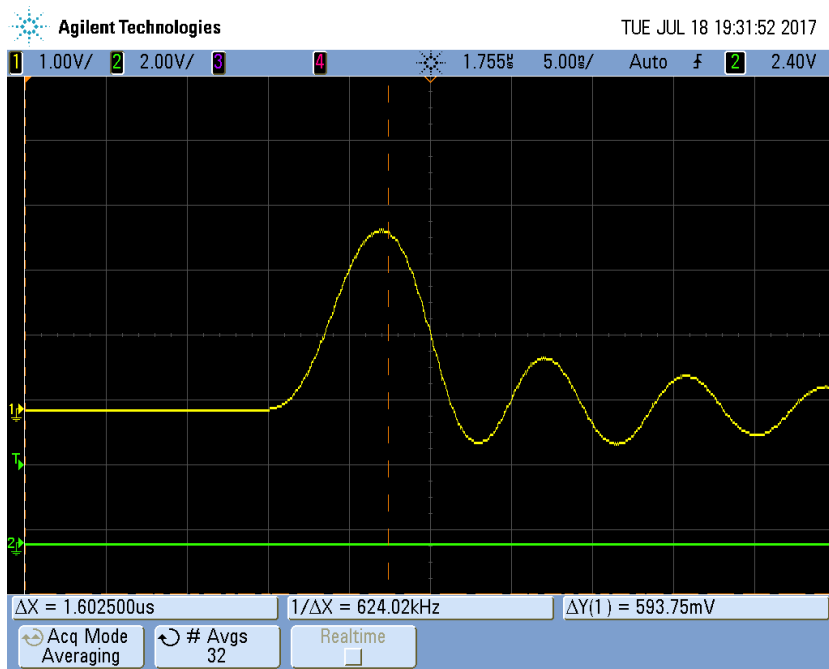


Figure 4.11: Peak voltage from FL and APD combination is 2.7 V

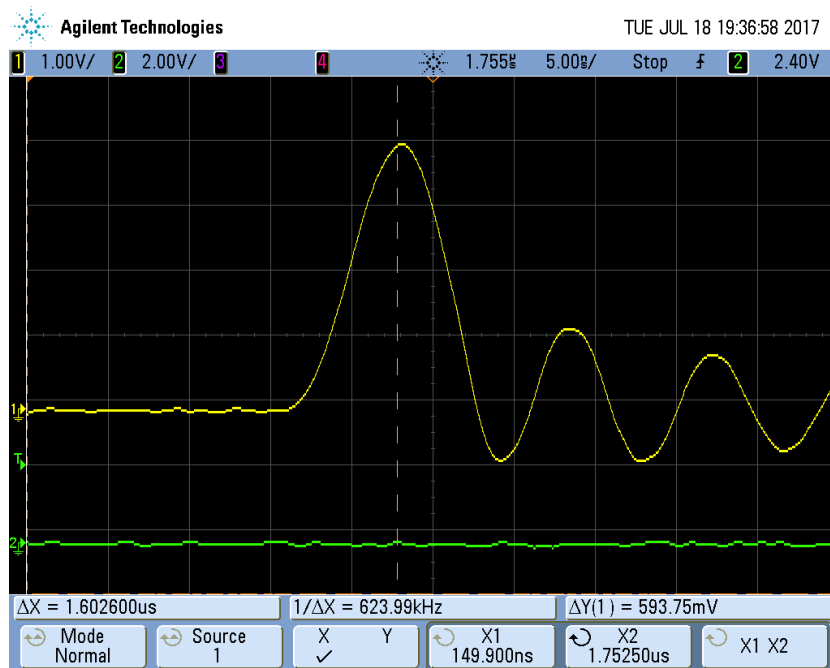


Figure 4.12: Minutes later the peak output signal is 4 V, without any noticeable change in weather. shows a maximum of 4 V of the returned pulse.

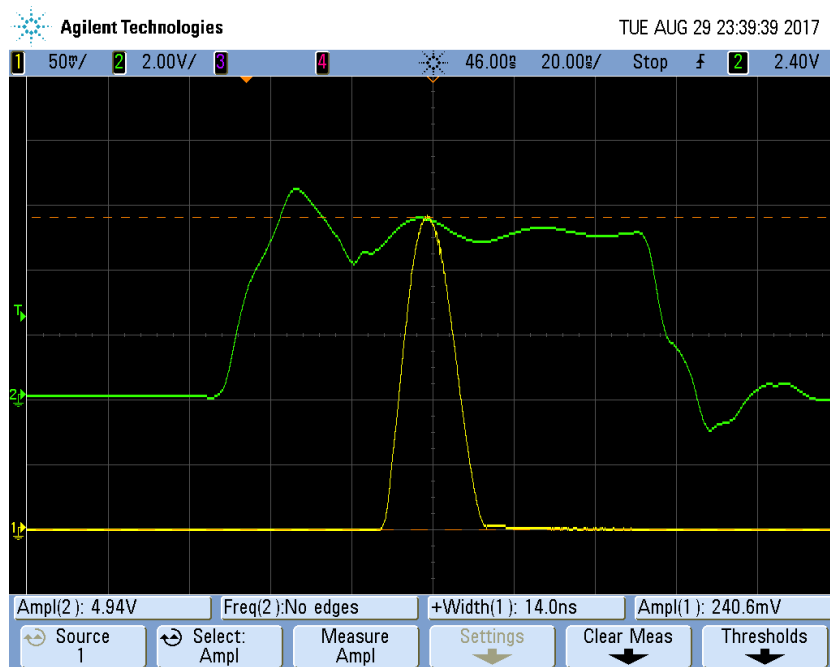


Figure 4.13: Returned pulse from LD and APD combination when holding a sheet of paper in front of laser.

Discussion

In general, there were a few challenges when doing the experimental testings. Originally, there was a 2nd retroreflector at a 1.5 km distance. This was taken down in the middle of the testing, and so, there were no valid results involving it. Having results from this would have been an advantage, as it would make it easier to compare with the theoretical range calculations to see how reliable they are.

The average power measured from the LF was found by using a thermal sensor. This makes the values more uncertain because the power measured will slowly increase with time. This was solved by waiting the same amount of time for every measurement, but this is not a perfect method. The FL itself had some issues. It could not give out the maximum power. The tip of the fiber connector was polished hoping that this would increase the output power, but it did not help. In addition to this, the output power would start to sway after being in use for some time, approximately 15 minutes. This would not show up on the multimeter monitoring the voltage consumption. This adds to the uncertainty of the returned power of the beam. The greatest challenges involved testing with the LD. To get a good result, the beam must be very well collimated, which is hard to achieve as there are many screws that can be adjusted to influence the beam. The behavior of the system during testing indicates that the beam was not collimated well enough. This would not have fixed everything, as the measured average output was 0.04 mW. This could come from many causes, the trigger pulse can have had the wrong frequency, the trigger pulse can have had too low voltage or be too short. Earlier, the average output power has been measured to be 1.6 mW, at 10 kHz using an other laser driver card, but this would not give the maximum pulse output either. The average power was measured using a thermal sensor. Unlike for the FL, the diode was not mounted to the detector in any way, and so some power could have leaked.

When asking for prices to estimate costs, there were a few companies that did

not reply in time, as it was in the middle of the summer vacation. It is also not easy to find suitable LD that could be used, and this makes the price selection small and could influence the cost estimate. When asking for prices, it was asked for the price per piece when buying a total of 50 pieces. The prices for SpotTrack is given per piece when buying 100 pieces. This Will rise the cost estimate. The cost estimate is only for changing the laser and detector. The real costs would include factors such as manufacturing and development, which could be different than for SpotTrack.

In the future, Er:glass microchip lasers should also be considered, as they can both reach high peak powers and have a lower price than a normal fiber laser. Currently, the pulse repetition rate is at a few Hz per second, and not suitable for this use.

Conclusion

We see that the range calculation for the different combinations all have potential to reach very far in clear weather. The combination with the best FOM was clearly the APD together with the FL. However, the safety considerations will not allow the FL to be operated at full power without any protective housing or other precautions. SpotTrack is rotating at 1 Hz, such a solution for the FL would help reduce the hazard. Table 3.6 Indicates that any solution involving the FL will be very expensive at this point. The APD is also very expensive compared to the pin detector, and so APD + FL is not an optimal solution. The same goes for the pin detector and FL combination. Even when using a pin detector in stead of an APD, this would still be a very expensive solution.

The data given in the data sheet gives a good indication of how the LD would perform in a system. Combined with the pin detector, the system does not perform better than SpotTrack and is twice as expensive. This would be a poor option for further development.

Combined with the APD, a system containing the LD will have a good range. The safety calculations showed that this system is eye safe on ranges further than 5 cm away from the collimating lens. This means that the laser can be operated at full power without any hazard. The FOM calculations gave a performance 30 times better than that of SpotTrack. The costs of this combination is 5 times that of SpotTrack. Based on the cost-FOM chart, this would the best option for further development.

Bibliography

- [1] Iselin Neteland. Further development of system for positioning/dp. 2017.
- [2] Naval Air Warfare Center Weapons Division. *Electronic Warfare & Radar Systems Engineering Handbook*. lulu.com, 2013.
- [3] H. Horvath. Atmospheric light absorption—a review. *Atmospheric Environment. Part A. General Topics*, 27(3):293–317, February 1993.
- [4] How to calculate laser beam size, February 2017.
- [5] The design of electro-optical sensors, 2009.
- [6] Adolph S. Jursa, editor. *Handbook of Geophysics and the Space Environment*. Air Force Geophysics Laboratory, 1985.
- [7] Internal documents at Kongsberg Seatex AS.
- [8] Rca. *Rca Electro-Optics Handbook*. RCA, 1974.
- [9] Hankwang at English Wikipedia. Mpe as energy density versus wavelength for various exposure times (pulse durations), 2007.
- [10] Laser Components. *High Intensity Pulsed Laser Diodes 1550 HI-Series*, 19 edition, July 16.
- [11] Keopsys. *Ultra/Compact Pulsed Laser Source User's Manual Model: KPS-KULT2-1550-028-007-020-SD-CO*.
- [12] Thorlabs. *PDA10CF(-EC) InGaAs Amplified Detector User Guide*, e edition, April 2015.
- [13] Thorlabs. *APD430x Operation Manual*, 1.1 edition, September 2015.
